J. Fluid Mech. (1996), *vol.* 311, *pp.* 239–255

On the stability of attachment-line boundary layers. Part 1. The incompressible swept Hiemenz flow

By RAY-SING LIN AND MUJEEB R. MALIK
High Technology Corporation, PO Box 7262, Hampton VA 23666, USA

(Received 15 February 1994 and in revised form 7 November 1995)

The stability of the incompressible attachment-line boundary layer is studied by solving a partial-differential eigenvalue problem. The basic flow near the leading edge is taken to be the swept Hiemenz flow which represents an exact solution of the Navier–Stokes (N–S) equations. Previous theoretical investigations considered a special class of two-dimensional disturbances in which the chordwise variation of disturbance velocities mimics the basic flow and renders a system of ordinary-differential equations of the Orr–Sommerfeld type. The solution of this sixth-order system by Hall, Malik & Poll (1984) showed that the two-dimensional disturbance is stable provided that the Reynolds number $\bar{R} < 583.1$. In the present study, the restrictive assumptions on the disturbance field are relaxed to allow for more general solutions. Results of the present analysis indicate that unstable perturbations other than the special symmetric two-dimensional mode referred to above do exist in the attachment-line boundary layer provided $\bar{R} > 646$. Both symmetric and antisymmetric two- and three-dimensional eigenmodes can be amplified. These unstable modes with the same spanwise wavenumber travel with almost identical phase speeds, but the eigenfunctions show very distinct features. Nevertheless, the symmetric two-dimensional mode always has the highest growth rate and dictates the instability. As far as the special two-dimensional mode is concerned, the present results are in complete agreement with previous investigations. One of the major advantages of the present approach is that it can be extended to study the stability of compressible attachment-line flows where no satisfactory simplified approaches are known to exist.

1. Introduction

Our investigation into attachment-line boundary-layer stability is stimulated by renewed interest in the design of laminar-flow swept wings in recent years. On a swept wing, it is known that multiple instability mechanisms can operate simultaneously to cause transition from laminar to turbulent flow. In flight tests, Gray (1952) was the first to observe that the boundary-layer transition on a swept wing occurred at a location much closer to the leading edge than that on a corresponding unswept wing. A decade later, further investigations of two pioneering Laminar Flow Control (LFC) programs, the X-21 (Pfenninger 1965) and British Handley Page (Gaster 1967), showed that once the turbulent attachment-line boundary layer had been established, suction systems deployed were not able to maintain the flow on the rest of the wing surface in the laminar state. This demonstrated that, from an LFC viewpoint, there is little point in considering other instability mechanisms if the attachment-line boundary layer is not laminar. Thus, the attachment-line boundary-layer stability represents a practical problem of great importance.

If the boundary-layer thickness is much smaller than the surface radius of curvature at the leading edge, the characteristics of the infinite swept attachment-line boundary-layer flow can be described by the classical Hiemenz flow (Rosenhead 1963) with the addition of a homogeneous spanwise velocity component. The resulting viscous layer is of constant thickness. One important feature of this flow is that it is an exact solution of the incompressible Navier–Stokes equations, not just the boundary-layer equations. This important feature allows a self-consistent stability analysis and a search for the critical Reynolds number. The term 'boundary layer' in this paper refers to the 'viscous layer' and does not imply the high Reynolds number approximation.

Poll (1978) made an attempt to predict the critical Reynolds number based on the parallel assumption; both chordwise (U) and wall-normal (V) velocity components of the basic flow were neglected so that the stability equations simply reduced to the classical Orr–Sommerfeld equation. The critical Reynolds number (R_θ) was predicted to be close to 270 based on momentum thickness along the attachment line. Later, Hall, Malik & Poll (1984, referred herein as HMP) made the first successful non-parallel stability analysis by studying a particular two-dimensional disturbance of the swept Hiemenz flow. They solved the linear stability equations obtained by assuming that the chordwise component of the perturbation velocity u' depends linearly on the chordwise coordinate x. The disturbance is a travelling Tollmien–Schlichting wave and can be written as

$$\{u', v', w'\} = \{xU(y), V(y), W(y)\} \exp[\mathrm{i}\beta(z - ct)], \tag{1}$$

where β is the spanwise wavenumber of the disturbance. They found the critical Reynolds number R_θ to be about 235 which is in good agreement with the experimental data of Pfenninger & Bacon (1969) and Poll (1979).

This particular x-dependence of the two-dimensional disturbance was first proposed and used by Görtler (1955) and Hämmerlin (1955) in studying the stability of two-dimensional stagnation-point flow. There was no *a priori* justification for making this assumption. The only reason for considering this type of disturbance is that variables become completely separable and governing equations reduce to more amenable ordinary differential equations. Wilson & Gladwell (1978) noted that the solutions studied by Hämmerlin could exhibit either exponential or algebraic decay away from the boundary layer. They further argued that disturbances arising in the boundary layer, without free stream forcing, should decay exponentially. If only the exponentially decaying disturbances are allowed, then the two-dimensional stagnation-point flow is found to be stable to all disturbances of the type described by (1). (For a more detailed discussion, the reader is referred to HMP.) Furthermore, for parallel flows, even though Squire's theorem shows that the critical Reynolds number is given by a two-dimensional disturbance, no equivalent theorem is known for swept Hiemenz flow. Only recently, the direct numerical simulation performed by Spalart (1988), for a single Reynolds number $R_\theta = 243$, gave support to the use of disturbances described by (1). Yet, the behaviour of three-dimensional disturbances has never been explored before, except in the asymptotic limit of large Reynolds number (Hall & Seddougui 1990).

It is now well known that the attachment-line boundary-layer flow is one of a few flows subject to subcritical instability, which means the instability may occur with finite-amplitude perturbations while linear theory predicts stability for all infinitesimal disturbances. This phenomenon was recognized as the leading-edge contamination problem in many previous investigations. Recently, two independent wind tunnel studies conducted by Poll & Danks (1995), and by Juillen & Arnal (1995) show that the turbulence propagating along the attachment line can be relaminarized by applying

surface suction. The result agrees well with the direct numerical simulations of Spalart (1988). Since the mechanisms behind attachment-line contamination and relaminarization are believed to be highly nonlinear, they are beyond the scope of this paper.

In this paper, we report on a generalized approach suited to studying the stability of attachment-line boundary layers. The approach is described here for incompressible flow but it is easily extendable to compressible flows. The stability is determined by solving the partial-differential eigenvalue problem resulting from the linearized stability equations. This is in contrast to previous investigations where a sixth-order ordinary-differential equation of the Orr–Sommerfeld type was used. The advantages of the method developed here can be summarized as follows:

(i) Neither the parallel assumption nor the restriction on disturbance is necessary, i.e. no prior knowledge about the solution is required.

(ii) Two- and three-dimensional disturbances can be studied simultaneously.

(iii) A number of low-instability modes are determined along with the most unstable mode.

(iv) The method is easily extendable to the compressible attachment-line flow with surface curvature effect, where, in general, the linear stability equations do not admit solutions in the form of (1).

Here we report results for the incompressible case to establish the applicability of this new approach. Results of this study place the use of (1) for incompressible stability on firm ground. We also show the existence of new instability modes which do not conform to (1). In §2 we describe the three-dimensional swept Hiemenz flow. In §3 we formulate the stability equations and present the solution techniques. Section 4 contains the results while the conclusions are drawn in §5.

2. Basic flow

For viscous incompressible flow over a swept body, the local solution in the vicinity of the attachment line can be represented by the swept Hiemenz flow if the boundary-layer thickness is small compared with the radius of the leading edge. Following the notation of HMP, the x-axis is taken to be the chordwise direction, the y-axis is in the direction normal to the surface, and the z-axis is in the spanwise direction, as shown in figure 1. The parameters of this flow are

$$\Delta = \left(\frac{\nu l}{U_0}\right)^{1/2}, \quad \bar{R} = \frac{W_0 \Delta}{\nu}, \tag{2}$$

where ν is the kinematic viscosity, l is a length scale in the x-direction, while U_0 and W_0 are independent velocity scales; Δ is the boundary-layer length scale, and $\bar{R}$ is the Reynolds number. The relationship between $\bar{R}$ and R_θ is $R_\theta = 0.404\bar{R}$. The swept Hiemenz solution is then given by

$$\bar{U} = \frac{\bar{U}^*}{W_0} = \frac{1}{\bar{R}} x\bar{u}(y), \quad \bar{V} = \frac{\bar{V}^*}{W_0} = \frac{1}{\bar{R}}\bar{v}(y), \quad \bar{W} = \frac{\bar{W}^*}{W_0} = \bar{w}(y), \tag{3}$$

where $x = x^*/\Delta$, $y = y^*/\Delta$ (asterisks represent the dimensional quantities), and $\bar{u}, \bar{v}, \bar{w}$ satisfy

$$\bar{u} + \bar{v}' = 0$$

$$\bar{v}''' + \bar{v}'^2 - \bar{v}\bar{v}'' - 1 = 0,$$

$$\bar{w}'' - \bar{v}\bar{w}' = 0,$$

$$\bar{v}'(0) = 0, \quad \bar{v}(0) = 0, \quad \bar{v}'(\infty) = -1, \quad \bar{w}(0) = 0, \quad \bar{w}(\infty) = 1.$$

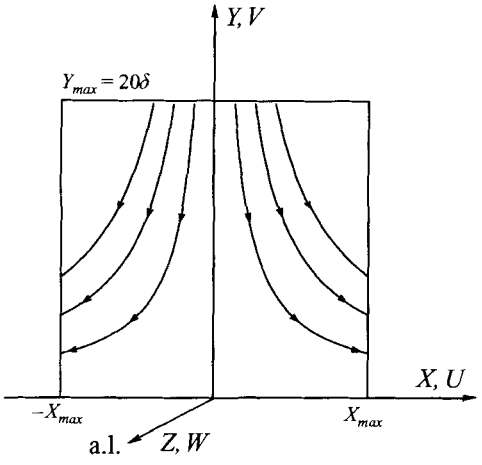

FIGURE 1. Coordinate system for attachment-line boundary-layer flow.

A simple shooting method, such as methods based on the Runge–Kutta formulae, can be used to solve the above equations in order to obtain the velocity profiles. The converged solution has $\bar{v}''(0) = -1.232587\,65$ and $\bar{w}'(0) = 0.570\,465\,25$. For more details about this swept Hiemenz solution, readers are referred to Rosenhead (1963).

3. Stability analysis

The derivation of the linear stability equations for the attachment-line boundary layer is rather straightforward. We consider infinitesimally small disturbances propagating along the attachment line, so that the instantaneous velocities u, v, and w and pressure p can be expressed as

$$q(x, y, z, t) = \bar{Q}(x, y) + q'(x, y, z, t), \tag{4}$$

where $q = (u, v, w, p)$, and barred and primed quantities represent basic-state and disturbance-state quantities, respectively. Substituting the above expression into the incompressible Navier–Stokes (N–S) equations, subtracting the basic state, and linearizing with respect to the small perturbations gives a set of linearized N–S equations which best describes the stability characteristics of small perturbations. In general, to solve this set of linearized N–S equations, which represents a set of partial different equations, is non-trivial. Therefore, in many studies the locally parallel assumption is routinely made to yield a reduced mathematical model which can be easily handled by the well-known normal-mode approach. However, it must be emphasized that in general there is no completely rational support for this parallel assumption, except for classes of flow such as plane Couette flow or Poiseuille flow. As pointed out earlier, HMP were able to treat the stability problem of the swept Hiemenz flow without the parallel flow approximation, but only for a special class of disturbances.

3.1. *The two-dimensional eigenvalue problem*

In this paper, we proceed from the linear N–S equations without making any further simplifications, and recognize that the problem consists of a set of coupled three-dimensional partial-differential equations with variable coefficients. These coefficients,

which depend on the basic flow, change strongly in the normal (y) direction and linearly in the chordwise (x) direction, but not in the spanwise (z) direction; see (3). As a consequence, the solution is separable in the variables z and t, and the disturbance quantities of a general travelling mode can be expressed in the form

$$q'(x,y,z,t) = \hat{q}(x,y)\exp[\mathrm{i}\beta(z-ct)] + \text{c.c.} \tag{5}$$

In this investigation, we only consider stability in the temporal sense. For a temporal stability formulation, β is real and represents the spanwise wavenumber, and c is the complex phase velocity whose real part represents the propagating speed of the disturbance in the spanwise direction and its imaginary part is proportional to the temporal growth rate. Then, the set of non-dimensional linear N–S equations can be written as

$$\frac{\partial\hat{u}}{\partial x}+\frac{\partial\hat{v}}{\partial y}+\mathrm{i}\beta\hat{w}=0, \tag{6a}$$

$$-\mathrm{i}\beta c\hat{u}+\bar{U}\frac{\partial\hat{u}}{\partial x}+\hat{u}\frac{\partial\bar{U}}{\partial x}+\bar{V}\frac{\partial\hat{u}}{\partial y}+\hat{v}\frac{\partial\bar{U}}{\partial y}+\mathrm{i}\beta\bar{W}\hat{u}=-\frac{\partial\hat{p}}{\partial x}+\frac{1}{\bar{R}}\left\{\frac{\partial^2\hat{u}}{\partial x^2}+\frac{\partial^2\hat{u}}{\partial y^2}-\beta^2\hat{u}\right\}, \tag{6b}$$

$$-\mathrm{i}\beta c\hat{v}+\bar{U}\frac{\partial\hat{v}}{\partial x}+\bar{V}\frac{\partial\hat{v}}{\partial y}+\hat{v}\frac{\partial\bar{V}}{\partial y}+\mathrm{i}\beta\bar{W}\hat{v}=-\frac{\partial\hat{p}}{\partial y}+\frac{1}{\bar{R}}\left\{\frac{\partial^2\hat{v}}{\partial x^2}+\frac{\partial^2\hat{v}}{\partial y^2}-\beta^2\hat{v}\right\}, \tag{6c}$$

$$-\mathrm{i}\beta c\hat{w}+\bar{U}\frac{\partial\hat{w}}{\partial x}+\bar{V}\frac{\partial\hat{w}}{\partial y}+\hat{v}\frac{\partial\bar{W}}{\partial y}+\mathrm{i}\beta\bar{W}\hat{w}=-\mathrm{i}\beta\hat{p}+\frac{1}{\bar{R}}\left\{\frac{\partial^2\hat{w}}{\partial x^2}+\frac{\partial^2\hat{w}}{\partial y^2}-\beta^2\hat{w}\right\}. \tag{6d}$$

All the quantities are scaled by the same set of reference parameters described in §2. Note that the introduction of the method of separation of variables reduces the three-dimensional linear partial-differential equations to two-dimensional ones in the x,y domain.

Similar to the plane Poiseuille flow, two fundamentally different types of solution are conceivable here. As far as the spanwise disturbance-velocity component is concerned, it is possible to have a symmetric solution, i.e. $\hat{w}(x,y)=\hat{w}(-x,y)$, and an antisymmetric solution, i.e. $\hat{w}(x,y)=-\hat{w}(-x,y)$. For the plane Poiseuille flow, it has been shown that the antisymmetric disturbances are always damped (Orszag 1971). However, for the attachment-line boundary-layer flow, no similar conclusion in this aspect has been reported before. As a matter of fact, our study finds that both symmetric and antisymmetric perturbations can be amplified in the attachment-line boundary layer. Results for both types of disturbances will be discussed in §4.

Before discussing the method of solving the system of equations, appropriate boundary conditions must be prescribed. The corresponding boundary conditions in the y-direction are

$$\hat{u}=\hat{v}=\hat{w}=0, \quad y=0,\infty \tag{7}$$

which assign zero-disturbance amplitudes to the solid surface ($y=0$) and at the far field ($y\to\infty$). In the x-direction, the boundary conditions for symmetric modes are

$$\hat{u}=\frac{\partial\hat{v}}{\partial x}=\frac{\partial\hat{w}}{\partial x}=0, \quad x=0, \tag{8a}$$

$$\hat{u}(x,y)=-\hat{u}(-x,y), \quad \hat{v}(x,y)=\hat{v}(-x,y), \quad \hat{w}(x,y)=\hat{w}(-x,y), \quad x=x_{max}. \tag{8b}$$

Note that, since $\hat{w}$ is symmetric with respect to the attachment line, which is assumed to be located at $x=0$, the $\hat{v}$ must also be symmetric and $\hat{u}$ must be antisymmetric such

that the continuity equation can always be satisfied. By the same token, the appropriate boundary conditions in the x-direction for antisymmetric modes are

$$\frac{\partial \hat{u}}{\partial x} = \hat{v} = \hat{w} = 0, \quad x = 0, \tag{9a}$$

$$\hat{u}(x,y) = \hat{u}(-x,y), \quad \hat{v}(x,y) = -\hat{v}(-x,y), \quad \hat{w}(x,y) = -\hat{w}(-x,y), \quad x = x_{max}. \tag{9b}$$

At this point, it may not seem clear how an oblique mode could be investigated by this method. Owing to the non-uniform nature of the Hiemenz flow in the x-direction, the method is aimed at studying the stability of an oblique Tollmien–Schlichting wave in the following form:

$$\begin{aligned} q'_R &= \hat{q}_R(x,y)\exp\left[\mathrm{i}\left(\int^x \alpha(\xi)\,\mathrm{d}\xi + \beta z - \omega t\right)\right] + \text{c.c.} \\ &= \hat{Q}_R(x,y)\,\mathrm{e}^{\mathrm{i}[\beta z - \omega t]} + \text{c.c.}, \end{aligned} \tag{10}$$

where $\hat{Q}_R(x,y) \equiv \hat{q}_R(x,y)\exp \mathrm{i}\int^x \alpha(\xi)\,\mathrm{d}\xi$. The above equation represents an oblique wave (i.e. a three-dimensional wave) propagating in both the positive x- and z-directions. (The two-dimensional mode, of course, corresponds to $\alpha(x) = 0$.) However, owing to the symmetry of the Hiemenz flow with respect to $x = 0$, it is conceivable that an identical disturbance propagating toward the negative x (still in the positive z) direction should also be possible. The linear combination of these two waves can be expressed as

$$\begin{aligned} f' &= \hat{Q}_R(x,y)\,\mathrm{e}^{\mathrm{i}[\beta z - \omega t]} + \hat{Q}_L(x,y)\,\mathrm{e}^{\mathrm{i}[\beta z - \omega t]} + \text{c.c.} \\ &= \hat{F}(x,y)\,\mathrm{e}^{\mathrm{i}[\beta z - \omega t]} + \text{c.c.}, \end{aligned} \tag{11}$$

where $\hat{F}(x,y) = \hat{Q}_R(x,y) + \hat{Q}_L(x,y)$. For a symmetric mode,

$$\left.\begin{aligned} \hat{Q}_R(x,y) = \hat{Q}_L(-x,y) &\to \hat{F}(x,y) = \hat{F}(-x,y) \quad \text{for} \quad v', w', p', \\ \hat{Q}_R(x,y) = -\hat{Q}_L(-x,y) &\to \hat{F}(x,y) = -\hat{F}(-x,y) \quad \text{for} \quad u'. \end{aligned}\right\} \tag{12}$$

Note that the linear combination does not alter the eigenvalue which could be either β or ω. Thus, for oblique modes, the eigenfunctions obtained by the current method actually represent the sum of a pair of oblique waves travelling, however, in different x-directions. We would like to emphasize that the effect of wavenumber $\alpha(x)$ is implicitly retained in the eigenfunction in this approach.

The computational domain is chosen to be enclosed by $(0 \leqslant y \leqslant y_{max})$ and $(-x_{max} \leqslant x \leqslant x_{max})$. The semi-infinite domain in y is truncated at $y = y_{max}$. Here y_{max} is the location where free-stream boundary conditions are satisfied, and $y_{max} = 20\delta$ is found adequate and is used throughout this paper. Similarly, the domain in the x-direction is truncated at $|x| = x_{max}$. At this moment, the selection of x_{max} is not clear since there is no obvious length scale in the x-direction. Numerical experiments show that the choice of x_{max} has a significant effect on the condition number of the resulting algebraic system of equations. It is found that with a given set of grids the resulting system of equations could have a prohibitively large condition number if x_{max} is chosen to be too small. Fortunately, the condition number drops quickly as x_{max} increases. A detailed discussion about the effect of x_{max} on the numerical solution will also be given in §4.

Equations (6*a–d*) together with their appropriate homogeneous boundary conditions form a two-dimensional partial differential eigenvalue problem. The numerical method used to discretize the equations and to ascertain eigenvalues will be discussed in the next section.

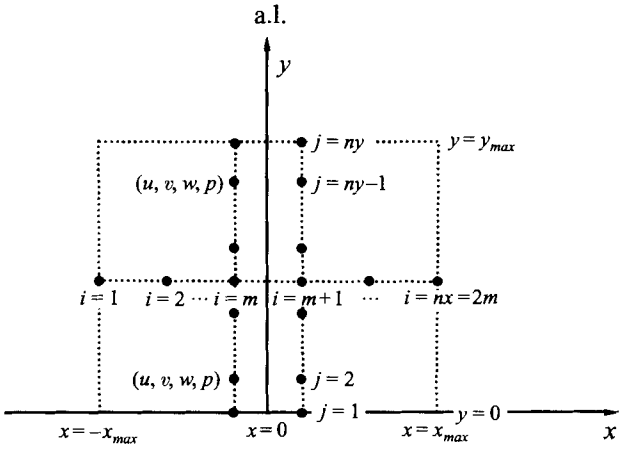

FIGURE 2. Grid and computational domain for attachment-line stability solutions of the two-dimensional partial-differential eigenvalue problem.

3.2. *Numerical method for two-dimensional stability equations*

We use the Chebyshev spectral collocation method for y-discretization of (6) and regular polynomials $\{P_n(x) = x^n, n = 0, 1, 2, \ldots\}$ for the x-discretization. An algebraic stretching is applied to map the physical domain in the wall-normal direction, $0 \leqslant y \leqslant y_{max}$, into the computational domain, $-1 \leqslant \xi \leqslant 1$, as well as to cluster points near the wall (see figure 2). The algebraic stretching is defined as

$$y = a\frac{1+\xi}{b-\xi}, \tag{13}$$

where $b = 1 + 2a/y_{max}$, and $a = y_i y_{max}/(y_{max} - 2y_i)$. This mapping will put half of the collocation points within the region $0 \leqslant y \leqslant y_i$. The collocation points in the computational plane are the Gauss–Lobatto points

$$\xi_j = \cos\frac{\pi(j-1)}{n_y - 1}, \quad j = 1, 2, \ldots, n_y. \tag{14}$$

In the x-direction, the spatial discretization employs uniformly distributed grid points:

$$x_i = -x_{max} + (i-1)\frac{2x_{max}}{n_x - 1}, \quad i = 1, 2, \ldots, n_x. \tag{15}$$

Now, the disturbance variable $\hat{q}$ can be represented as the double series

$$\hat{q}(x, y) = \sum_{n=0}^{n_x-1} \sum_{k=0}^{n_y-1} c_{n,k} P_n(x) T_k(\xi), \tag{16}$$

where the P_n are the regular polynomials referred to above and T_k the Chebyshev polynomials of degree k. In the x-direction, both symmetric and antisymmetric solutions (with respect to the attachment line) are possible. For symmetric (even) solutions, all of the coefficients with n odd vanish identically, i.e. $c_{n,k} = 0$ for n odd. Conversely, the expansions with $c_{n,k} = 0$ for n even are antisymmetric (or odd). It is convenient to choose n_x even so that $n_x = 2m$. Equation (16) can then be written as

$$\hat{q}(x, y) = \sum_{n=0}^{m-1} \sum_{k=0}^{n_y-1} c_{2n,k} P_{2n}(x) T_k(\xi) \tag{17}$$

for even solutions, and

$$\hat{q}(x,y) = \sum_{n=0}^{m-1} \sum_{k=0}^{n_y-1} c_{2n+1,k} P_{2n+1}(x) T_k(\xi) \tag{18}$$

for odd solutions. With the above even and odd expansions, the symmetric and the antisymmetric boundary conditions in the x-direction can be satisfied automatically.

In the y-direction, if all the collocation points are used for all the dependent variables, i.e. $(\hat{u}, \hat{v}, \hat{w}, \hat{p})$, then the discrete linear system will be underdetermined. Therefore, two extra artificial compatibility conditions must be imposed at $y = 0$ and $y = y_{max}$. Here, we use Neumann conditions on pressure as

$$\left(\frac{\partial \hat{p}}{\partial y}\right)_{y=0} = X_0, \tag{19}$$

$$\left(\frac{\partial \hat{p}}{\partial y}\right)_{y=y_{max}} = X_M, \tag{20}$$

where X_0 and X_M are evaluated by using the normal momentum equation and the continuity equation at the two boundaries. These two extra boundary conditions are needed because we have not used a staggered grid as described by Malik, Zang & Hussaini (1985). The spatial derivatives of $\hat{q}$ at collocation points are accomplished by matrix operations. The derivative matrices can be computed either by directly differentiating the interpolating polynomial constructed on the set of collocation points or by means of a transform method (see Canuto *et al.* 1987).

The governing equations in the discrete sense can be represented as a generalized algebraic eigenvalue problem of the form

$$\boldsymbol{A}\boldsymbol{x} = c\boldsymbol{B}\boldsymbol{x}, \tag{21}$$

where the $\boldsymbol{A}$ matrix is complex, full, non-Hermitian, while the $\boldsymbol{B}$ matrix is real, diagonal, and singular. With $n_x(=2m)$ and n_y collocation points in the x- and y-directions, respectively, the order of the complex matrix eigenvalue problem is $4n_y m$. This indicates that even with a moderate spatial resolution, the order of the matrix can easily reach a few thousands. Thus the two-dimensional eigenvalue problem is quite a challenge compared to the one-dimensional problem. Here, the eigenvalue c is determined by using the QR matrix eigenvalue algorithm (Wilkinson 1965). The approach is to first form $\boldsymbol{A}^{-1}\boldsymbol{B}$ followed by reducing $\boldsymbol{A}^{-1}\boldsymbol{B}$ to Hessenberg form $\boldsymbol{H}$, and then find all the eigenvalues $(1/c)$ of $\boldsymbol{H}$ by QR iteration. The advantage of this method is that a number of low-instability modes are determined along with the most unstable mode. The disadvantages are that the number of operations and computer storage needed to determine the eigenvalues are extensive.

4. Results and discussion

A systematic grid study has been carried out to determine an appropriate spatial resolution in the x–direction such that converged solutions can be achieved by the present partial-differential eigenvalue approach. Our experience of the one-dimensional analysis corresponding to that of HMP indicated that $y_{max} = 20\delta$ and $n_y = 43$

n_x	c_r	c_i ($\times 10^2$)	Mode
4	0.35840982	0.58532472	S1
	0.35791970	0.40988668	A1
	0.36002184	0.19923199	A2*
8	0.35840982	0.58532472	S1
	0.35791970	0.40988668	A1
	0.35743540	0.23430007	S2
	0.35695687	0.058571260	A2
12	0.35840982	0.58532472	S1
	0.35791970	0.40988668	A1
	0.35743540	0.23430006	S2
	0.35695687	0.058571269	A2

TABLE 1. The effect of the chordwise resolution on eigenvalues of swept Hiemenz flow for $\bar{R} = 800$, $\beta = 0.255$, and $x_{max} = 11\delta$; * denotes that the solution is not converged

	Symmetric modes			Antisymmetric modes		
x_{max}	c_r	c_i ($\times 10^2$)	Rcond	c_r	c_i ($\times 10^2$)	Rcond
8δ	0.35840982	0.58532472	3.1×10^{-6}	0.35791970	0.40988667	5.7×10^{-6}
	0.35743540	0.23430008		0.35695687	0.058571289	
4δ	0.35840982	0.58532465	5.4×10^{-7}	0.35791970	0.40988657	7.9×10^{-7}
	0.35743540	0.23430008		0.35695687	0.058571555	
2δ	0.35840953	0.58526147	4.1×10^{-8}	0.35791997	0.40987375	4.7×10^{-8}
	0.35743555	0.23443775		0.35695625	0.58571304	
δ	0.35828997	0.63922098	1.8×10^{-9}	0.36056275	0.036414497	1.2×10^{-9}
	0.35829179	0.10723099		0.35364430	0.031523171	

TABLE 2. Effect of x_{max} on computed eigenvalues for $\bar{R} = 800$, $\beta = 0.255$, $y_{max} = 20\delta$, $n_y = 43$, and $n_x = 12$. Rcond = reciprocal of the L1 condition number of $\boldsymbol{A}$.

constitute a set of satisfactory parameters. Our major interest here is focused on finding their counterparts in the x–direction. In table 1, we document all of the unstable eigenvalues computed here for $\bar{R} = 800$, $\beta = 0.255$, and $x_{max} = 11\delta$. Results indicate that the two-dimensional eigenvalue method requires only four chordwise collocation points ($n_x = 4$, or $m = 2$) to have converged first symmetric (S1) and the first antisymmetric (A1) modes, up to eight significant digits. With $n_x = 8$, the second symmetric (S2) and antisymmetric (A2) modes are also fully resolved. However, no other unstable modes were found by further increasing the chordwise resolution up to $n_x = 24$. In all our subsequent calculations, results show that the most unstable mode is always the first symmetric (S1) mode and the temporal growth rates of different modes follow the relation, S1 > A1 > S2 > A2 > S3 > ..., without exception. Another interesting observation is that unstable modes with identical spanwise wavenumber always travel with very similar phase speeds. The phase speed increases slightly as the growth rate goes up, but the difference is typically less than 0.5%. The linear interaction between modes having comparable phase speeds can give rise to disturbances in the form of modulated wave packets, which have been recorded by the hot-wire measurements of Pfenninger & Bacon (1969) in laminar attachment-line boundary layers.

To study the effect of the x-domain size on the computed solutions, a series of computations has been carried out with all the parameters fixed except the x_{max}. Results are summarized in table 2. This shows that the condition number of matrix $\boldsymbol{A}$

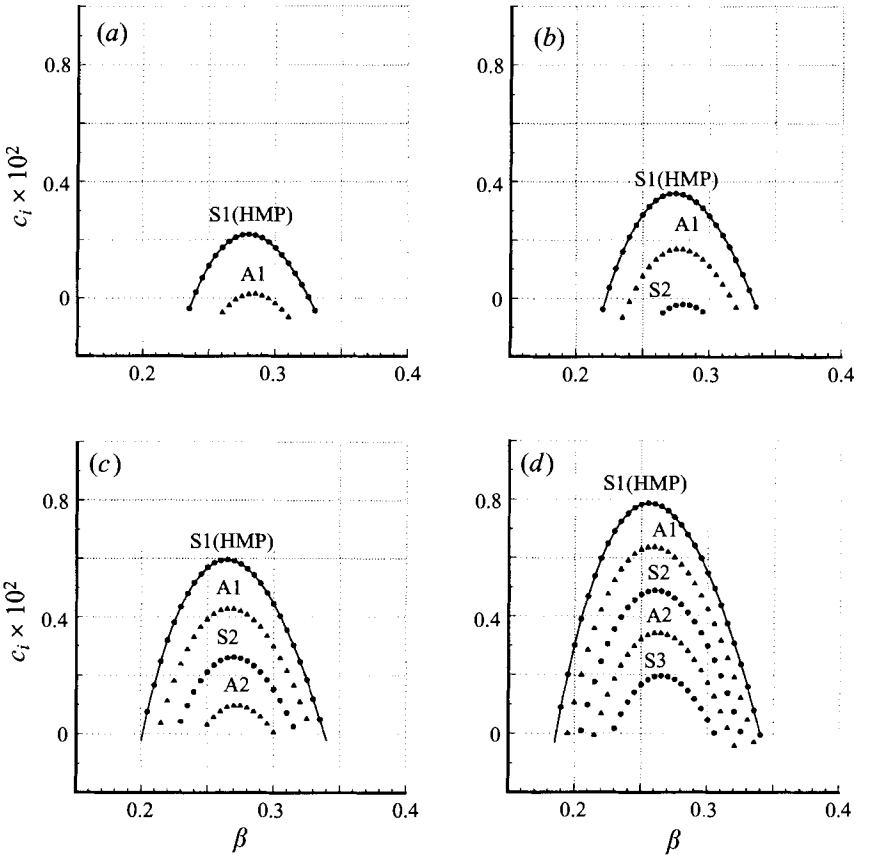

FIGURE 3. Variation of c_i of symmetric and antisymmetric disturbances for swept Hiemenz flow at (*a*) $\bar{R} = 650$, (*b*) 700, (*c*) 800 and (*d*) 900. Solid lines: HMP solution; symbols: current results, ●, symmetric; △, antisymmetric.

is a function of x_{max}; its magnitude increases as x_{max} decreases. Consequently, the once-converged eigenvalue begins to lose significant digits as the chordwise computational domain shrinks. Under the parameters considered in table 2, when $x_{max} < 2\delta$, the condition number of matrix $\boldsymbol{A}$ becomes so large that eigenvalues are fully contaminated by round-off errors. (All of the computations were performed on a CRAY Y-MP using single precision.) Evidence from further numerical experiments shows that as long as x_{max} is chosen to be greater than 2δ, converged solutions up to at least 6 significant digits can be achieved.

Stability analyses for Reynolds numbers ($\bar{R}$) equal to 650, 700, 800, and 900 have been performed by using the present two-dimensional eigenvalue approach. Figure 3 shows the variation of temporal growth rate c_i as a function of spanwise wavenumber β. Also plotted in this figure are results obtained by using the linear stability theory of HMP. Extensive results have been reported by HMP using the method based on the disturbance described by (1). Since those solutions are mathematically admitted by the linear N–S equations, they serve as a check for the two-dimensional eigenvalue technique used here. The comparison indicates that the first symmetric mode (S1) computed by the present two-dimensional eigenvalue approach fully recovers the solution of HMP. This provides a solid validation of our two-dimensional eigenvalue method.

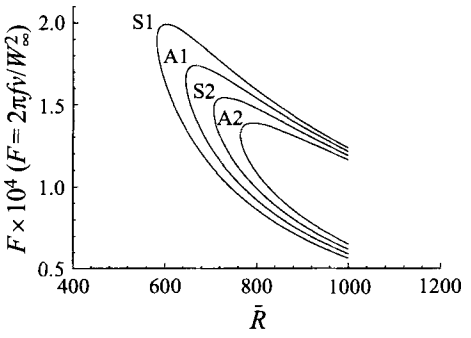

FIGURE 4. Neutral curves for S1, A1, S2, and A2 modes of the swept Hiemenz flow.

In addition to the HMP solution, as the Reynolds number exceeds 650, the first unstable antisymmetric disturbance (A1 mode) emerges from below. For $\bar{R} = 900$, four extra branches of unstable waves (A1, S2, A2, S3) coexist with the HMP solution, and the growth rate of the A1 mode is comparable to the most unstable S1 mode. It is conceivable that more branches of unstable travelling waves will arise as the Reynolds number becomes even higher. The neutral curves of these modes are given in figure 4. The critical Reynolds numbers from these curves are 583, 646, 707 and 765 for S1, A1, S2 and A2 modes, respectively. Clearly, the lowest critical Reynolds number is determined by the HMP solution. This again places the use of disturbances of (1) in the study of incompressible attachment-line boundary-layer stability on firm ground. A similar conclusion has also been drawn by the direct numerical simulation performed by Spalart (1988). His simulation was performed at $\bar{R} = 600$ ($R_\theta = 243$) at which only the HMP (or S1) mode remains unstable according to the present analysis. As mentioned above, the linear interaction between unstable modes can create modulated wave packets. These modulated wave packets were first observed at $\bar{R} = 636$, in the experiment conducted by Pfenninger & Bacon (1969). This is in good agreement with the critical Reynolds number of the A1 mode which is about 646 as shown in figure 4.

Comparisons of the disturbance amplitude functions in the (x, y)-plane are given in figure 5(*a*, *b*). All the solutions are normalized in such a way that the maximum value is 1. It can be seen that the amplitude of $\hat{u}$ decays more quickly than the other two velocity components. This has been shown by HMP through examining the asymptotic behaviour of solutions at large y. As shown in figure 5(*a*), the $\hat{w}$ and $\hat{v}$ amplitude functions of the S1 mode show absolutely no variation with x, as suggested by (1). On the other hand, for the rest of the unstable modes discovered here, disturbances off the attachment line consistently have larger amplitudes than those on the attachment line itself. By placing another hot wire 0.5 in. off the attachment line, Pfenninger & Bacon (1969) also observed a much larger spanwise ($\hat{w}$) velocity fluctuation than that registered by the hot wire right on the attachment line, even when the perturbation amplitude was as small as 0.1%. This experimental observation strongly suggests the existence of the low-instability modes discovered here. Interestingly, the growth of these disturbances with x suggests that nonlinearity will first appear away from the attachment line.

A close examination of disturbance-amplitude functions in the (x, y)-plane reveals that among all of the unstable modes discovered here, only the S1 mode (HMP solution) truly represents a separable solution of (6*a–d*). To illustrate this point, without losing generality, we assume that $\hat{u}$ is separable and can be expressed as

$$\hat{u} = X(x)\, Y(y) = x^m \tilde{u}(y),$$

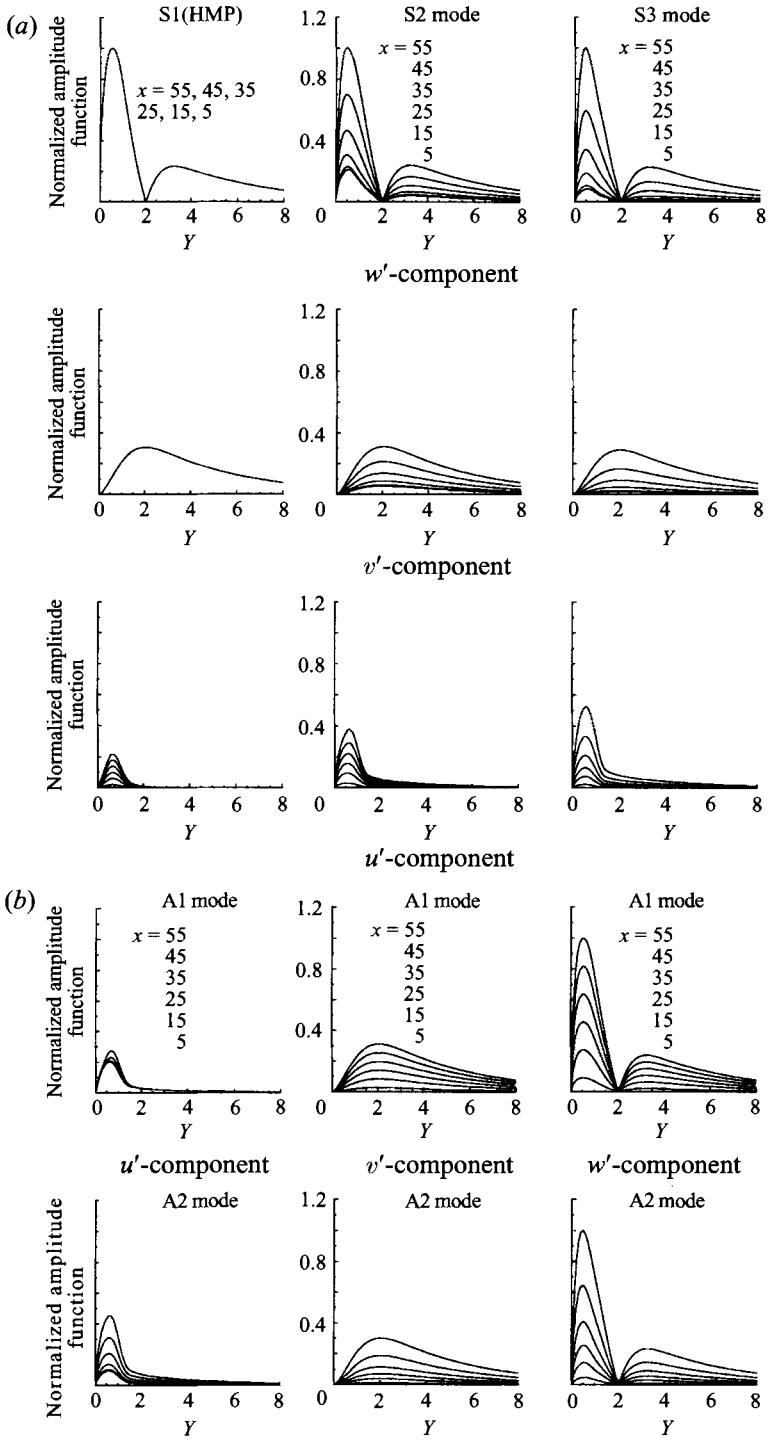

FIGURE 5. The distribution of normalized eigenfunctions for $\bar{R} = 900$, $\beta = 0.255$; (*a*) symmetric modes; (*b*) antisymmetric modes. The magnitude of eigenfunctions at various x stations increases with x.

where m must be determined by satisfying the governing equations and by permitting a complete separation of variables. From the continuity equation, the other two velocity components must be proportional to x^{m-1}. Furthermore, if the pressure amplitude function is assumed to be

$$\hat{p} = x^{m_p}\tilde{p}(y),$$

then it can be shown that the x-dependency cannot be completely removed from the momentum equations except for the very special case of $m = 1$ and $m_p = 0$, for which the separable solution studied by HMP is recovered.

Figure 6(*a*, *b*) shows the phase relations in the (x, y)-plane. It can be seen that except for the S1 mode, all other modes display different degrees of phase variation in the x-direction. In other words, the S1 mode represents the only true two-dimensional disturbance, while other modes clearly are three-dimensional disturbances. However, the first antisymmetric mode (A1) can easily be mistaken for a two-dimensional wave if only phase information at one side of the attachment line is gathered in experiments. This is best illustrated by figure 7, which shows wavefront geometries of spanwise disturbances in the (x, z)-plane at a fixed y. This capability of studying both two- and three-dimensional disturbances simultaneously makes the two-dimensional eigenvalue method an effective tool for future compressible attachment-line applications, for which three-dimensional disturbances are expected to be the most relevant disturbances.

As mentioned before, the attachment-line boundary-layer flow is known to be subject to sub-critical instability. As suggested by Landau (1944), there should be a global critical Reynolds number, below which all disturbances, infinitesimal and finite, decay ultimately. Experiments show that for attachment-line flow the global critical Reynolds number is about $\bar{R} = 250$ (Pfenninger 1965; Gaster 1967; Poll 1978; Arnal & Juillen 1989), which is much lower than that given by the linear stability theory. Hall & Malik (1986) performed a weakly nonlinear and numerical analysis based on the two-dimensional disturbance (S1 mode) and reported a subcritical limit of $\bar{R} \approx 530$. Clearly, the gap between this two-dimensional calculation and the experimental results is still very wide. Hall & Seddougui (1990) used triple-deck theory coupled with the high-Reynolds-number approximation to investigate the stability of three-dimensional modes, and used weakly nonlinear theory to study their interaction with the two-dimensional disturbance. Their results show that the interaction causes the de-stabilization of the two-dimensional mode and is responsible for the breakdown of the two-dimensional modes at a finite distance from the attachment line. Therefore, it seems that three-dimensionality may be the dominant factor in the above-mentioned discrepancy. What role the three-dimensional modes discovered here may play in the subcritical instability might be worth exploring.

To provide an idea about how these unstable disturbances would affect the flow structure, a three-dimensional instantaneous velocity field is constructed according to the formula

$$g(x, y, z) = \bar{G}(x, y) + \tau\,\mathrm{Re}[\hat{g}(x, y)\,\mathrm{e}^{\mathrm{i}\beta z}], \tag{22}$$

where $g = (u, v, w)$, and τ is a free parameter which controls the magnitude of the disturbance. Here τ is chosen in such a way that

$$\mathrm{Max}\,(w'(x, y, z)) = 0.2\,\overline{W}_0. \tag{23}$$

The disturbance is chosen to be either the S1 mode or A1 mode. To gain insight into the velocity field, the particle-trace technique is used to visualize the flow structure.

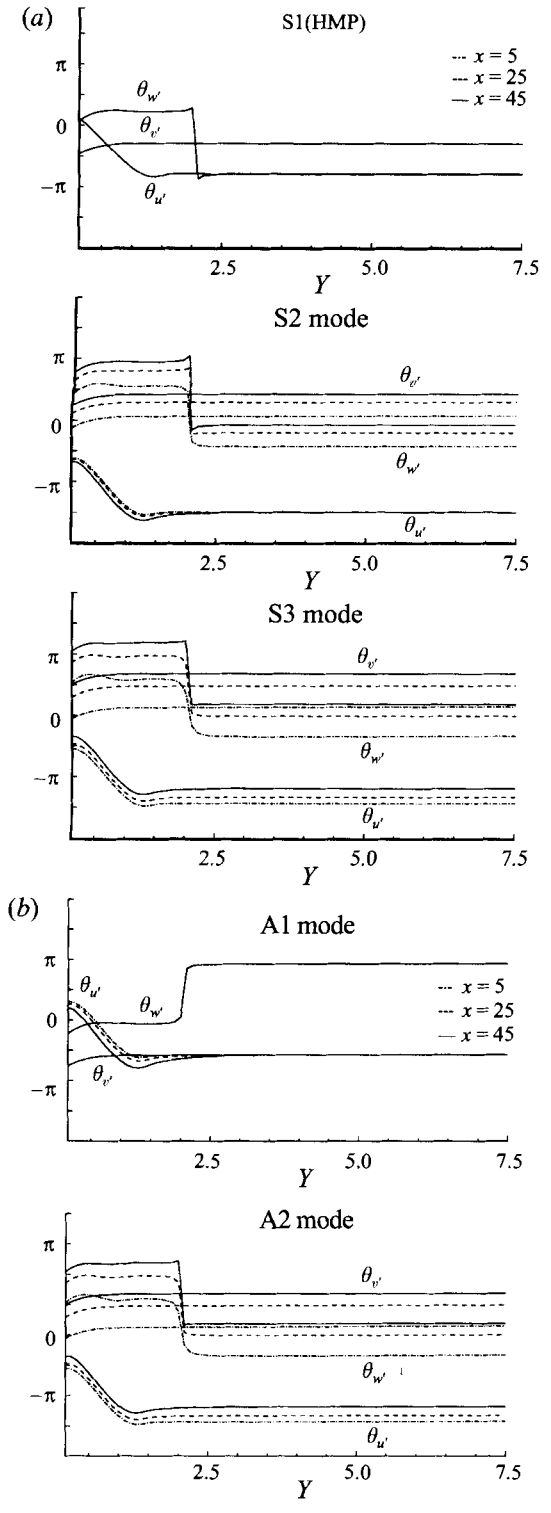

FIGURE 6. The phase relationship of unstable disturbances of (*a*) symmetric, and (*b*) antisymmetric modes at $\bar{R} = 900$ and $\beta = 0.255$.

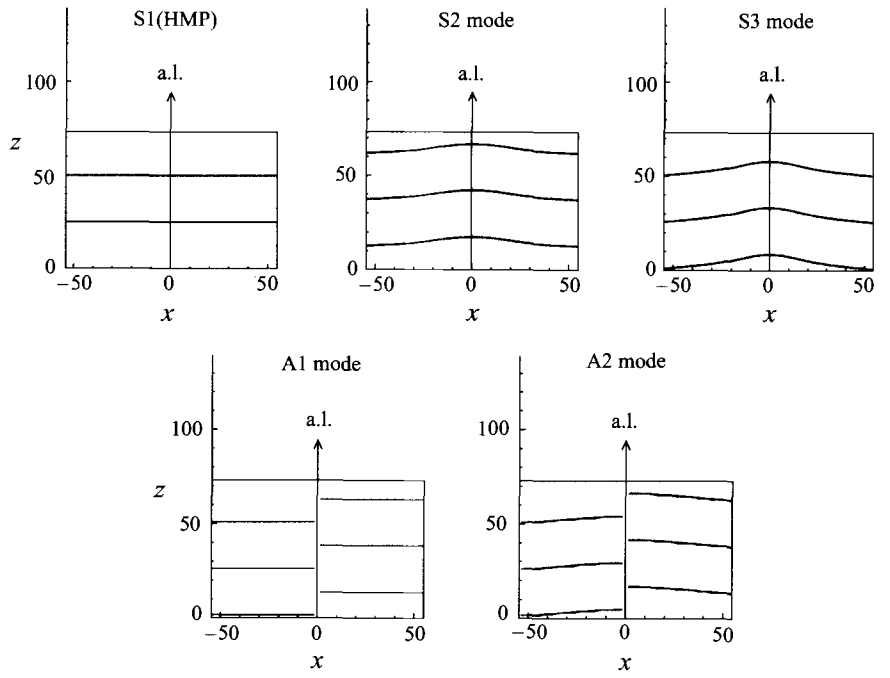

FIGURE 7. The wavefront geometries of spanwise velocity disturbances at $\bar{R} = 900$ and $\beta = 0.255$, in the (x, z)-plane at a fixed y.

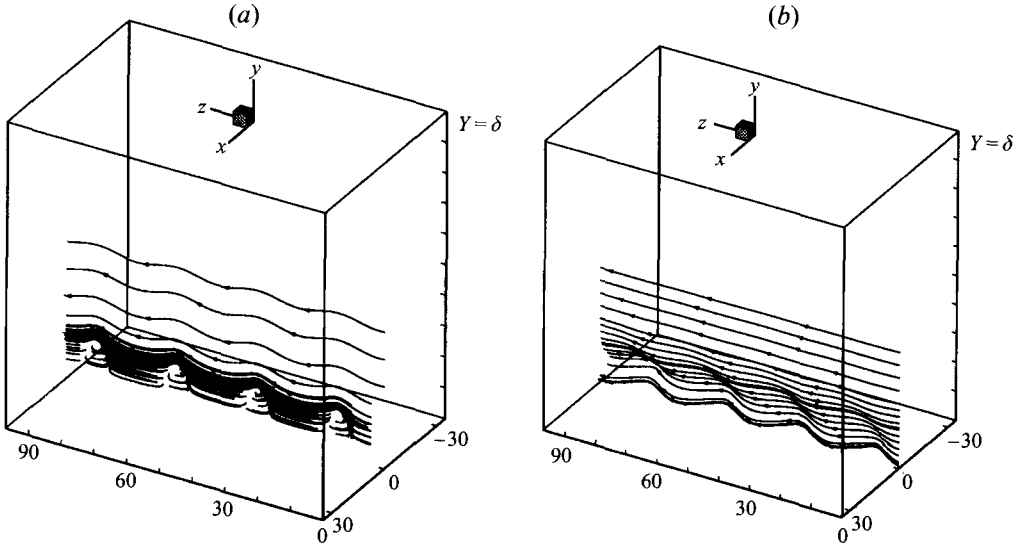

FIGURE 8. Computed particle trace of the attachment-line flow under the influence of the two most dangerous disturbances: (*a*) S1 modes; (*b*) A1 mode.

Results are shown in figure 8(*a*, *b*). It can be seen that the attachment line remains straight under the influence of a symmetric disturbance. The vortex structure has its axis in the chordwise direction, as shown in figure 8(*a*). On the other hand, an antisymmetric disturbance makes the attachment line wind back and forth across the highlight, see figure 8(*b*). These particle-trace pictures provide a qualitative depiction

of the attachment-line boundary-layer flow in the presence of symmetric and antisymmetric modes.

5. Conclusion

The stability of incompressible attachment-line boundary layers has been studied by using the two-dimensional eigenvalue approach, in which the linearized partial differential stability equations are solved numerically. The particular mean flow is taken to be the swept Hiemenz flow which represents an exact solution to the Navier–Stokes equations. According to the previous result of HMP, a two-dimensional symmetric travelling disturbance was known to be unstable for this flow, and the critical Reynolds number was found to be $\bar{R} = 583.1$. In this paper, using the present approach, new travelling modes have been identified for $\bar{R} > 646$. These new modes can be split into two major categories, symmetric and antisymmetric. We have shown that both symmetric and antisymmetric modes can be amplified by the swept attachment-line boundary layer. However, the most unstable mode is found to be the two-dimensional symmetric disturbance considered earlier by HMP. These new low-instability modes are mainly three-dimensional travelling waves with phase speed very close to that of the most unstable two-dimensional wave. There appears to be some experimental evidence (Pfenninger & Bacon 1969) which supports the existence of these modes; however, further studies (both experimental and computational) are needed to investigate the characteristics of these modes and, particularly, their role in the attachment-line boundary-layer transition.

Results of the present study show that the two-dimensional eigenvalue approach can be a very effective tool for examining the stability characteristics of more general attachment-line boundary layers than the swept Hiemenz flow. This study also builds confidence in directly extending the current method to the stability analysis of compressible attachment-line boundary layers where the linear stability problem cannot be studied by simplified approaches previously used for incompressible flows.

On a typical swept wing, driven by the favourable pressure gradient near the leading edge, the boundary-layer flow accelerates away from the attachment line and shortly enters the crossflow instability region. A possible connection between attachment-line and crossflow instabilities had been suggested by Hall & Seddougui (1990). By choosing a computational domain large enough in the x-direction to cover both the attachment-line instability and crossflow instability regions, and by using an appropriate spatial resolution, the two-dimensional eigenvalue approach can provide us with a means to explore this connection. However, this extension might not be trivial and it would require the development of relatively more sophisticated numerical techniques for solving eigenvalues of very large non-Hermitian matrices.

This work was sponsored under NASA Contracts NAS1-19299 and NAS1-20059, Langley Research Center.

REFERENCES

ARNAL, D. & JUILLEN, J. C. 1989 Leading edge contamination and relaminarization on a swept wing at incidence. *4th Symp. on Numerical and Physical Aspects of Aerodynamic Flows* (ed. T. Cebeci). Springer.

CANUTO, C., HUSSAINI, M. Y., QUARTERONI, A. & ZANG, T. A. 1987 *Spectral Methods in Fluid Mechanics*. Springer.

GASTER, M. 1967 On the flow along swept leading edges. *Aero. Q.* **18**, 165–184.

GRAY, W. E. 1952 The effect of wing sweep on laminar flow. *RAE TM* 255. Royal Aircraft Establishment, Farnborough, UK.

GÖRTLER, H. 1955 Dreidimensionale Instabilität der ebenen Staupunkt-Strömung gegenüber wirbelartigen Störungen. In *Fifty Years of Boundary Layer Research* (ed. H. Görtler & W. Tollmien), p. 304. Vieweg und Sohn.

HALL, P. & MALIK, M. R. 1986 On the instability of a three-dimensional attachment-line boundary layer: weakly nonlinear theory and a numerical approach. *J. Fluid Mech.* **163**, 257–282.

HALL, P., MALIK, M. R. & POLL, D. I. A. 1984 On the stability of an infinite swept attachment line boundary layer. *Proc. R. Soc. Lond.* A **395**, 229–245.

HALL, P. & SEDDOUGUI, S. O. 1990 Wave interactions in a three-dimensional attachment-line boundary layer. *J. Fluid Mech.* **217**, 367–390.

HÄMMERLIN, G. 1955 Zur Instabilitätstheorie der ebenen Staupunktströmung. In *Fifty Years of Boundary Layer Research* (ed. H. Görtler & W. Tollmien), p. 315. Vieweg und Sohn.

JUILLEN, J. C. & ARNAL, D. 1995 Experimental study of boundary layer suction effects on leading edge contamination along the attachment line of a swept wing. *Laminar-Turbulent Transition* (ed. R. Kobayashi), p. 173. Springer.

LANDAU, L. D. 1944 On the problem of turbulence. *C.R. Acad. Sci. URSS* **44**, 311–314.

MALIK, M. R., ZANG, T. A. & HUSSAINI, M. Y. 1985 A spectral collocation method for the Navier-Stokes equation. *J. Comput. Phys.* **61**, 64–88.

ORSZAG, S. A. 1971 Accurate solution of the Orr–Sommerfeld stability equation. *J. Fluid Mech.* **50**, 689–703.

PFENNINGER, W. 1965 Flow phenomena at the leading edge of swept wings. Recent developments in boundary layer research-Part IV. *AGARDograph* 97, May 1965.

PFENNINGER, W. & BACON, J. W. 1969 Amplified laminar boundary layer oscillations and transition at the front attachment line of a 45° flat-nosed wing with and without boundary layer suction. In *Viscous Drag Reduction* (ed. C. S. Wells). Plenum.

POLL, D. I. A. 1978 Some aspects of the flow near a swept attachment line with particular reference to boundary layer transition. *College of Aeronautics Rep.* 7805.

POLL, D. I. A. 1979 Transition in the infinite swept attachment line boundary layer. *Aero. Q.* **30**, 607.

POLL, D. I. A. & DANKS, M. 1995 Relaminarisation of the swept wing attachment-line by surface suction. *Laminar–Turbulent Transition* (ed. R. Kobayashi), p. 137. Springer.

ROSENHEAD, L. 1963 *Laminar Boundary Layers*, pp. 467–75. Oxford University Press.

SPALART, P. R. 1988 Direct numerical study of leading edge contamination. *AGARD CP* 438.

WILKISON, J. 1965 *The Algebraic Eigenvalue Problem.* Oxford University Press.

WILSON, S. D. R. & GLADWELL, I. 1978 The stability of a two-dimensional stagnation flow to three-dimensional disturbances. *J. Fluid Mech.* **84**, 517–527.